

Investigation of poppet valve vibration with cavitation

Kento Kumagai^a, Shohei Ryu^a, Masanori Ota^b and Kazuo Maeno^c 

^aResearch Division Technical Research Center, Hitachi Construction Machinery Co., Ltd., Kandatsu-Machi, Tsuchiura, Ibaraki, Japan; ^bDivision of Artificial Systems Science, Graduate School and Faculty of Engineering, Chiba University, Yayoi-Cho, Inage-Ku, Chiba, Japan; ^cKisarazu National College of Technology, Kiyomidai-Higashi, Kisarazu, Chiba, Japan

ABSTRACT

The poppet valve is a popular component in hydraulic systems, but it is also well known as trouble maker because it may occasionally induce unpredictable vibration. In former previous studies it has been found that cavitation is an important reason for this kind of vibration, but the causal mechanism between the vibration and cavitation is unclear. In this study, we developed a visualisation experiment system, in which we can observe and analyse the dynamic relationship among the displacement of the poppet, the cavitation quantity and the pressures around the poppet in a visualisation experiment. Based on the observation of the experimental phenomena and data analysis, we propose a hypothesis of a mechanism that can explain how cavitation influences the vibration of the poppet valve.

ARTICLE HISTORY

Received 15 February 2015
Accepted 28 October 2015

KEYWORDS

Cavitation; hydraulic;
poppet valve; vibration;
visualisation

1. Introduction

Poppet valves are one of the most popular components of hydraulic systems and are used as check valves, relief valves, and flow control valves because of their high responsiveness and low pressure loss. However, poppet valves sometimes induce vibration and noise in a system (Weaver 1980). Even poppet valves with identical or similar structures may perform well in one system and vibrate in another. In addition, when a valve for which a problem has been reported is taken back to the factory, it may show stable performance. The vibration of a poppet valve is difficult to predict because it has many causes and the reproduction of the phenomenon is difficult.

Many researchers have studied the vibration of poppet valves. Lutz (1933) investigated the relationship between poppet valve vibration and the surrounding volume, finding that destabilisation is caused by a delay resulting from the compressibility of the hydraulic oil. Backé and Rünneburger (1964) analysed the behaviour of poppet valves in circuits including peripheral equipment and pipes, and reported that coupling of the valve with other components such as a pump can also destabilise the poppet valve. Maeda (1970) reported that the cause of transverse vibration is an unstable flow force acting on the poppet valve. Later, Hayashi (1995) investigated the behaviour of a wide range of systems including the collision between the valve seat and the valve, revealing that various nonlinearities affect poppet valve vibration.

We have also been conducting research focusing on the vibration generated in the specific conditions of the poppet valve. Our previous investigations revealed a peculiar vibration of the valve that occurs in the case of cavitation, which cannot be predicted according to only the pulsation of peripheral components and self-vibration induced by the pipe line in numerical simulations (Kumagai *et al.* 2014a). In addition, we revealed that it is possible to predict the trend of the vibration by assuming the change in the bulk modulus of the hydraulic oil base on the mixing of cavitation bubbles in numerical analysis (Kumagai *et al.* 2014b). This finding is important in terms of its technical utility because of the possible evaluation of the poppet valve vibration accompanying cavitation by approximation of the effects of cavitation by the bulk modulus. However, what is the actual state of the flow field? How is the cavitation related to the vibration of the poppet valve? These questions have not yet been answered.

Accordingly, in the present study, to target the poppet valve vibration in the cavitation state confirmed in the previous report (Kumagai *et al.* 2014a), we observed the poppet valve vibration phenomenon with cavitation by measuring it with a visualisation experimental apparatus and a high-speed camera, and investigated the correlation between the state of cavitation, pressure and poppet displacement. Furthermore, we investigated the cause of the change in the flow field focusing on the quantity of bubbles and the state of the vortex. Finally, we formulated a possible generation mechanism of the poppet

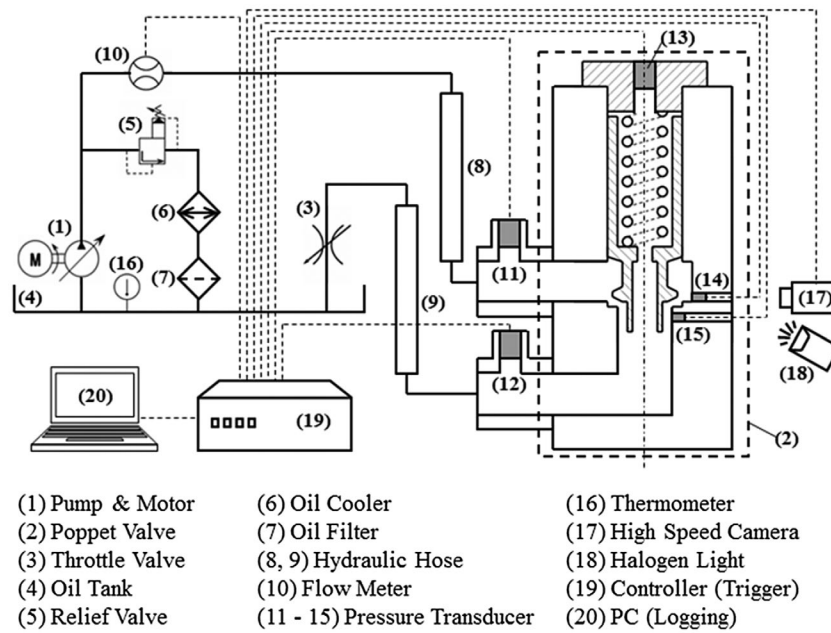


Figure 1. Experimental system.

valve vibration with cavitation according to these results. From the results of the visualisation experiments, we are able to deduce the relationship between the vibration of a poppet valve and cavitation.

2. Experimental system and measurement

2.1. Experimental system

The experimental system is shown in Figure 1 and comprises a variable-displacement axial piston pump (1) (where the number of pistons in the pump N was nine and the rotational speed of the pump n was 1500 min^{-1}), the tested poppet valve (2), a variable throttle valve (3) for adjusting the pressure downstream of the tested valve, and an oil tank (4). These components were connected with hydraulic rubber hoses (8 and 9). In another circuit, a relief valve (5) that prevents abnormal pressure in the hydraulic circuit (the set pressure of the relief valve was 10 MPa and the valve did not open under the experimental conditions), an oil cooler (6) that adjusts the oil temperature, and an oil filter (7) were connected to the oil tank.

The structure and size of the tested poppet valve in the experiment are given in Figure 2. The tested valve consisted of a transparent housing (21) that was made of the acrylic resin polymethylmethacrylate, a poppet (22) made of S45C steel (the mass of the poppet m was about 0.1 kg), a spring (23) with a spring constant k of 21 N/mm, and a plug (24). A convergent flow-type poppet was used to facilitate observation of the state of cavitation and poppet movement. This poppet had an effective pressure receiving area A_{pu} in the location indicated in red in Figure 2, and the force due to the upstream pressure was less susceptible to the dynamic pressure near the opening portion. Moreover, because the pressure of the

spring chamber avoids the effect of the dynamic pressure near the opening portion, the guide indicated in blue in Figure 2 was set on the poppet. The sliding part between the poppet and the housing L_{slide} was long enough to prevent lateral vibration of the poppet. The valve seat of the housing had a sharp edge, and the parallel portion between the valve seat and poppet was negligible. The spring chamber (25) consisted of the poppet, the acrylic block and the plug connected to the downstream flow path; the pressure of the spring chamber was almost the same as the downstream pressure.

2.2. Measurement system

A high-speed video camera (17) (Keyence Co., Ltd, VW-9000) and a metal halide lamp (18) were used to measure the movement of the poppet valve. The high-speed camera and metal halide lamp were positioned vertical to the poppet centre axis. The imaging conditions were a frame rate of 6000 fps and an electron shutter speed of $1/16,000 \text{ s}$, and the images were recorded using a monochromatic lens. Pressure was measured by pressure transducers (Kyowa Electronic Instruments Co., Ltd, PGL-A-5MP-A) placed upstream (11), downstream (12) and in the spring chamber (13) of the valve. The specifications of these pressure transducers (11)–(13) were a response frequency of 12.2 kHz and a resolution of 0.005 MPa. Additionally, under some conditions, upstream (14) and downstream (15) pressures were measured by pressure transducers (FISO Technologies Inc., FOP-M-BA) placed from the valve seat to a distance of 2.5 mm. The specifications of these pressure transducers (14) and (15) were a response frequency of 15 kHz and a resolution of 0.0136 MPa. The rate of flow (10) passing through the poppet valve was measured by a gear flow meter (Kracht GmbH, VG1BKP2S61)

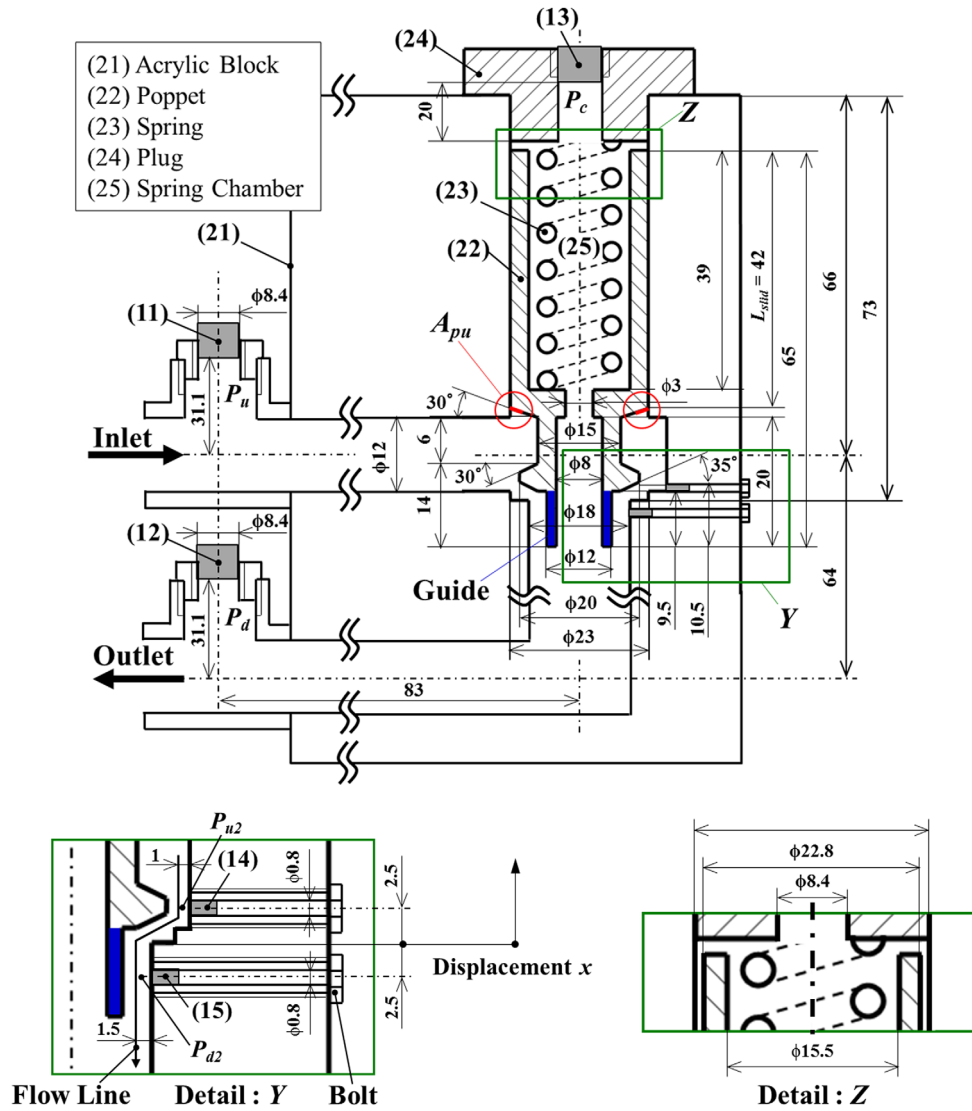


Figure 2. Tested poppet valve.

upstream of the poppet valve. The oil temperature was measured by a thermometer (16) in the oil tank. The high-speed video camera, flow meter and pressure transducers were connected to a controller (19), and began measuring at the same time after receiving a trigger from the controller. Logging data were recorded on a personal computer (20) at a sampling frequency of 10 kHz. The dynamic displacement of the poppet valve was measured by processing the image data from the high-speed video camera; the displacement was obtained by taking the difference between the still image at any time and a standard image in a state in which the poppet was seated.

2.3. Experimental conditions

The experimental conditions investigated are given in Table 1. The oil was a mineral oil-based hydraulic fluid with an ISO viscosity grade of 46. The working conditions for the tested poppet valve were mainly determined by two factors: the flow rate of the pump Q and the downstream average pressure $P_{d_{ave}}$. In the main experiment, we fixed T at 40 ± 2 °C, and changed Q from 10 to

50 ± 1.5 L/min in intervals of 10 L/min. For all flow conditions, we adjusted $P_{d_{ave}}$ as 0.05 MPa. $P_{d_{ave}} = 0.05$ MPa when the throttle valve was fully open, and it varied with a flow rate in the range $0.01 \leq P_{d_{ave}} \leq 0.10$ MPa. However, the flow rate is considered to be $P_{d_{ave}} = 0.05$ MPa for the sake of convenience in this study. When observing the vortex of the downstream, the oil temperature was set at $T = 30 \pm 2$ °C to facilitate observation of the bubbles and vortex. We recorded the flow rate, pressure and image data, which were processed to identify the dynamic displacement of the poppet valve.

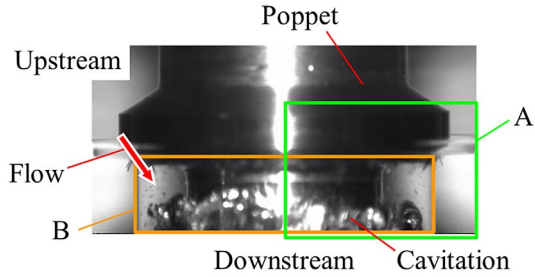
3. Experimental results and discussion

3.1. Flow state in downstream of the poppet valve

First, we investigated the flow state downstream when the poppet valve was vibrating in the cavitation state. Figure 3 shows a still image from the video taken by the high-speed camera at $Q = 10$ L/min and $T = 30 \pm 2$ °C. The black part in the centre of the image is the poppet valve,

Table 1. Experimental conditions.

Quantity	Symbol	Value	Units
Downstream average pressure	$P_{d,ave}$	0.05	MPa (Gauge)
Pump flow rate	Q	10, 20, 30, 40, 50 \pm 1.5	L/min
Oil temperature	T	30, 40 \pm 2	$^{\circ}$ C
Kinetic viscosity	ν	4.547×10^{-5}	$m^2/s @ 40^{\circ}C$
Oil density	ρ	868.9	kg/m^3
Viscosity index		109	

**Figure 3.** Image taken by the high speed camera at $Q = 10\text{L/min}$ and $T = 30^{\circ}C$.

the white part downstream of the poppet valves illustrates cavitation bubbles, and the red arrows indicate the flow direction of the fluid. The portion A and B within the frame is the inspection area for observation and image processing, which will be described later. Figure 4 shows still images for $Q = 10\text{L/min}$ and $T = 30^{\circ}C$ in temporal order; these indicate the same position as portion A in Figure 3. The number in the images indicates the time t for each frame.

In Figure 4, we found that cavitation bubbles are generated near the valve seat ($t = 2/6000\text{ s}$), a bubble cluster forms in the annular flow after the cavitation bubbles away from the valve seat ($t = 3/6000\text{ s}$), the bubble cluster flows downstream ($t = 3/6000 - 9/6000\text{ s}$), and the bubbles hardly exist in the downstream portion of the image ($t = 10/6000\text{ s}$). Focusing on the bubble movement of the portion surrounded by the circle ($t = 3/6000\text{ s}$), we can confirm that the bubble on the outside of the bubble cluster of annular flow moves back from the downstream to the valve seat ($t = 3/6000 - 5/6000\text{ s}$), and flows again to the downstream by changing its direction ($t = 6/6000 - 7/6000\text{ s}$). This means that vortex flow exists downstream, and the bubble cluster in the annular flow is formed by this vortex involving the cavitation bubbles.

From the results, when the poppet valve is vibrating in the cavitation state, we found that the annular vortex is generated downstream, and this vortex is released further downstream.

3.2. Correlation of cavitation and poppet vibration

Since the cavitation and vortex of the state downstream was revealed in the previous section, we investigate the relationship between those and the poppet displacement in this section. Note that the condition in the previous

section was $T = 30^{\circ}C$ to make it easy to observe the behaviour of the cavitation bubbles. However, the condition in this section is $T = 40 \pm 2^{\circ}C$ to investigate the correspondence between this and the previous report (Kumagai *et al.* 2014b).

Figure 5 shows still images for $Q = 30\text{L/min}$ and $T = 40^{\circ}C$ in temporal order. Figure 6 shows the displacement of the poppet x obtained by image processing. The conditions are the same as those for Figure 5, and time t is synchronised with the time of each frame in Figure 5.

In Figure 5, a large quantity of cavitation has been generated in the downstream portion. Furthermore, the presence of the annular vortex flow can be confirmed by the behaviour of the cavitation bubbles, which are indicated by frames of broken lines and dot-dashed lines. The annular vortex is consistent with the phenomenon that has been identified in Section 3.1. We find that an annular vortex was released into the downstream twice while the valve vibrated once. The first release of the annular vortex occurred when the poppet was close to the valve seat ($t = 1/6000 - 3/6000\text{ s}$), while the second release occurred immediately after the poppet reached maximum displacement ($t = 6/6000 - 8/6000\text{ s}$). In addition, the cavitation bubbles momentarily disappeared after the second release of the annular vortex ($t = 10/6000\text{ s}$). This means that two states a liquid-phase and multi-phase were present in the flow field and the switching between them was instantaneous. Figure 6 shows that the phenomenon in Figure 5 occurred during one cycle of poppet valve vibration.

Upon obtaining this result, we verified whether there was a continuous matching of the poppet vibration period and switching cycle of the flow field state. First, we represent the quantity of the cavitation bubbles in the numerical value by obtaining the average brightness value B_{ave} ($0 \leq B_{ave} \leq 255$) under each conditions. Here, B_{ave} is defined as the average brightness of the pixels in the inspection area B as shown in Figure 3. B_{ave} correlates with the quantity of cavitation bubbles because the cavitation bubbles appear white by reflecting light, which is related to an increase in B_{ave} . B_{ave} is the brightness of the image rather than the intensity of light, and it does not have a unit. However, since the reflected light is affected by many factors other than the quantity bubbles, B_{ave} cannot represent the quantity of bubbles exactly. Therefore, we discuss only the qualitative trend of the quantity of the cavitation bubbles by B_{ave} .



Figure 4. Flow state in downstream for $Q = 10\text{ L/min}$ and $T = 30\text{ }^\circ\text{C}$. These images are the portion A in Figure 3.

Figure 7(a)–(e) presents the relationship between the brightness of the inspection area B (quantity of cavitation bubbles) and displacement of the poppet at $Q = 10\text{--}50\text{ L/min}$ and $T = 40\text{ }^\circ\text{C}$. The blue and red plots respectively show the poppet displacement x and the average brightness B_{ave} . The dashed black line indicates the brightness when the inspection area is completely in the liquid phase. We found that B_{ave} continued to oscillate together with x , having a period consistent with that of x under the condition $Q = 10\text{--}50\text{ L/min}$. The phase of B_{ave} was approximately opposite that of x under the condition $Q = 10\text{ L/min}$, shifted slightly at $Q = 20\text{ L/min}$, offset by about one-quarter of the wavelength from the opposite phase at $Q = 30$ and 40 L/min , and the opposite phase of x again at $Q = 50\text{ L/min}$. Furthermore, under the condition $Q = 10\text{--}40\text{ L/min}$, for which there was severe vibration of the poppet, B_{ave} reduced momentarily near $B_{ave} = 78$. This means that there was switching to the liquid-phase from the multi-phase state. Because B_{ave} was always larger than

$B_{ave} = 78$ at $Q = 50\text{ L/min}$, the multi-phase state of the flow field was retained at all times by the cavitation bubbles.

The above results show that, under the conditions for which there was poppet valve vibration with cavitation, the quantity of cavitation bubbles fluctuated owing to a large fluctuation of the flow field as the field switched from the multi-phase to the liquid-phase. Moreover, the waveform of the poppet displacement and the quantity of cavitation bubbles were offset by one-quarter of the wavelength from the opposite phase.

3.3. Transient state of cavitation bubbles and pressure

In response to the results obtained in the previous section, we speculated that the disappearance of the cavitation cloud indicates an increase in pressure in the flow field. The disappearance of cavitation is related to an increase in pressure because cavitation strongly depends

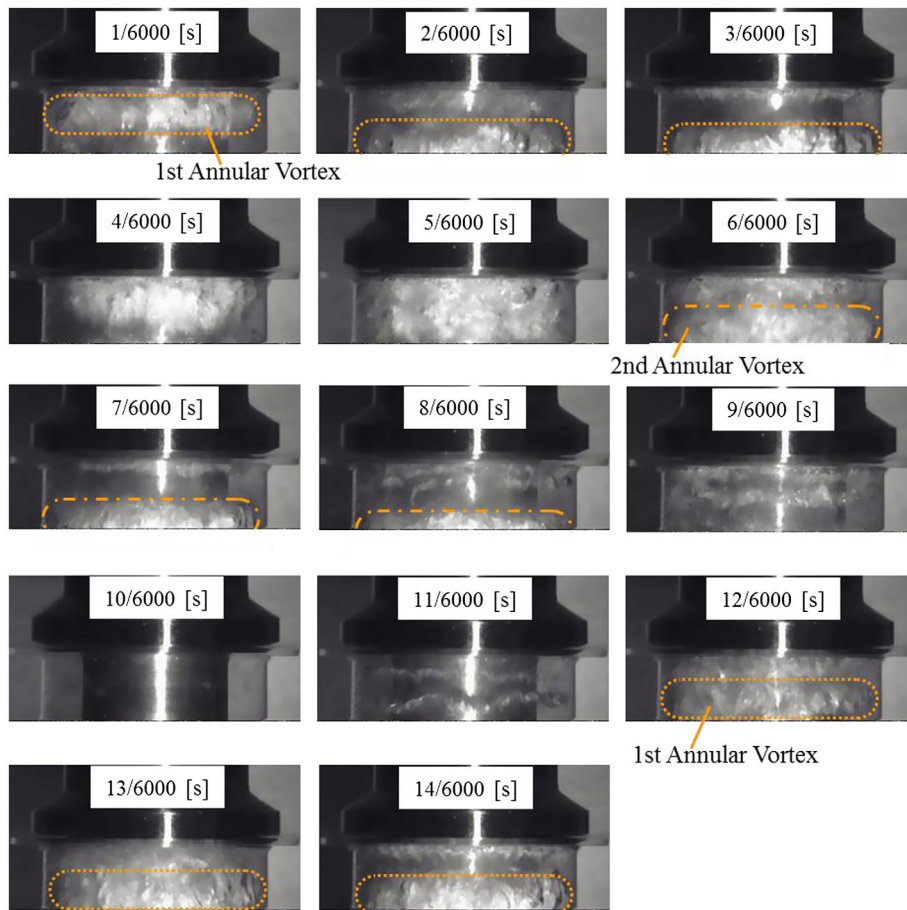


Figure 5. Transient state of cavitation for $Q=30\text{L/min}$ and $T=40\text{ }^\circ\text{C}$.

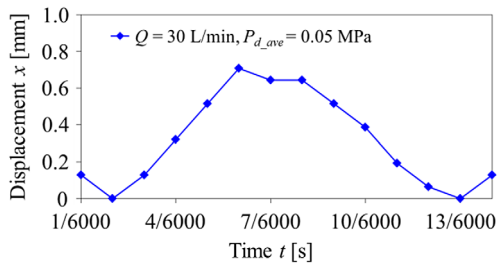


Figure 6. Displacement of the poppet at $Q=30\text{L/min}$ and $T=40\text{ }^\circ\text{C}$.

on pressure (Knapp *et al.* 1970). Accordingly, to test this hypothesis, we conducted measurements by installing pressure transducers in the immediate vicinity of the seat portion, denoted (14) and (15) in Figure 1.

Figure 8 shows the correlation between factors at $Q=20\text{L/min}$ and $T=40\text{ }^\circ\text{C}$; the factors presented are (a) upstream pressure P_{u2} , downstream pressure P_{d2} and spring chamber pressure P_c , (b) poppet displacement x and average brightness B_{ave} of the inspection area (quantity of cavitation bubbles), and (c) force acting on the poppet F calculated from the measurements. The dashed lines indicate the intervals of data taken by the high-speed camera. F is calculated as

$$F = A_{pu}P_{u2} + A_{pd}P_{d2} - A_{pc}P_c - K(x + x_i) \quad (1)$$

where the pressure receiving area A_{pu} is 157 mm^2 , A_{pd} is 249 mm^2 , A_c is 406 mm^2 , the spring constant k is 21 N/mm and the initial compression of the spring is 11.2 mm . Figure 9 presents the state of cavitation corresponding to the frame number in Figure 8.

From Figure 8(a) and (b), we find that, while the poppet made one vibration, P_{u2} , P_{d2} and P_c fluctuated as follows. P_{u2} increased suddenly in the period beginning with the poppet seated and ending at the maximum of x at (frames 1–4), decreased rapidly in frames 4–7 and recovered slowly in frames 7–10. P_{d2} reached an initial peak when the poppet was seated (frame 1), reached a first minimum in frame 3, increased again in frames 3–5 and reached a second peak in frame 5, reduced slowly in frames 5–9 and reached a second minimum in frame 9. P_c fluctuated little between frames 1 and 10.

Focusing on the relationship between B_{ave} and each factor, we find that B_{ave} had a high value in frames 1–4, a minimum value in frame 5 and a comparatively low value in frames 6–10. This means that cavitation bubbles were generated and expanded in the process of the poppet opening with a rapid increase in P_{u2} , bubbles disappeared when x and P_{d2} took maximum values, and the quantity of cavitation bubbles was less in the process of the poppet closing with a rapid decrease in P_{u2} . Figure 9 shows the occurrence of cavitation and the release of

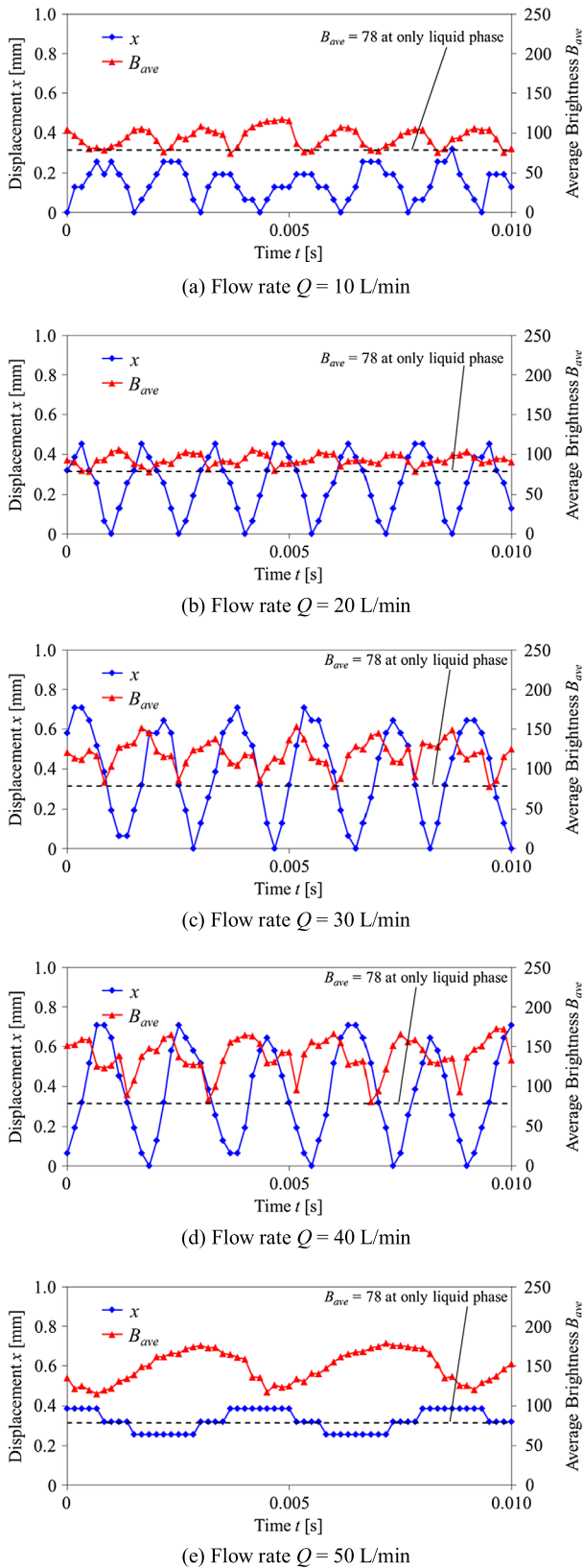


Figure 7. Relationship between the brightness of the inspection area (quantity of cavitation bubbles) and the displacement of the poppet at $T=40$ °C; (a) $Q=10$ L/min, (b) $Q=20$ L/min, (c) $Q=30$ L/min, (d) $Q=40$ L/min and (e) $Q=50$ L/min. The blue and red plots respectively show the poppet displacement x and the average brightness B_{ave} . The dashed black line indicates the brightness when the inspection area is completely in the liquid phase.

the annular vortex in frames 1–4, and the subsequent, disappearance of cavitation bubbles in frame 5.

Next, focusing on the relationship between F and each factor, we find that P_{u2} dominantly acted on the poppet movement, because the waveform of F was similar to that of P_{u2} . This means that P_{u2} was the direct cause of the vibration, and the underlying cause of the vibration was the factor that produced a fluctuation in P_{u2} .

From the results described above, we have focused on the influence of cavitation on the discharge coefficient of the poppet valve, as reported by Oshima and Ichikawa in 1986. Since the actual flow rate is less than the theoretical flow rate, a cross-sectional area of the throttle portion of the poppet valve corresponding to the actual flow rate $C_d A(x)$ is calculated according to

$$C_d A(x) = Q \sqrt{\frac{\rho}{2(P_{u2} - P_2)}} \quad (2)$$

where $A(x)$ is the opening area of the poppet that is calculated by the displacement, and C_d is the discharge coefficient. Since C_d is the ratio between the theoretical flow rate and the actual flow rate, it includes the influence of cavitation. Therefore, C_d changes depending on the state of the cavitation, and the change will affect the upstream pressure under the condition of constant flow.

In Figure 8 and Equation (2), the relationship between the quantity of cavitation bubbles and upstream pressure is described. Specifically, in the opening process of the poppet with a large quantity of cavitation bubbles, it is difficult for the fluid to flow by a reduction in C_d . In the closing process with fewer cavitation bubbles, the fluid flows easily by recovery of C_d . In other words, the pressure increases excessively in the opening process and decreases rapidly in the closing process with the fluctuation in the quantity of cavitation bubbles. Therefore, the fluctuation in the quantity of cavitation bubbles is regarded as the underlying cause of the vibration.

The above conclusion means that the downstream pressure is important, because the quantity of cavitation bubbles has a strong correlation with the downstream pressure. Therefore, we next consider the behaviour of the downstream pressure. As shown in Figure 8, we confirm that P_{d2} is at a maximum value in frame 5 when B_{ave} is at a minimum value. This result means that the increase in downstream pressure extinguishes cavitation. Here, we consider the cause of the downstream pressure increase. In Figure 9, the annular vortex is released downstream before the cavitation bubbles disappear in frames 1–3. This is likely caused by the poppet displacement sweeping away the vortex. Therefore, after the vortex is released, space is formed between the released vortex and the poppet opening, and the oil flows from upstream into this space. However, since the oil is inhibited in its flow by the released vortex, the pressure rises

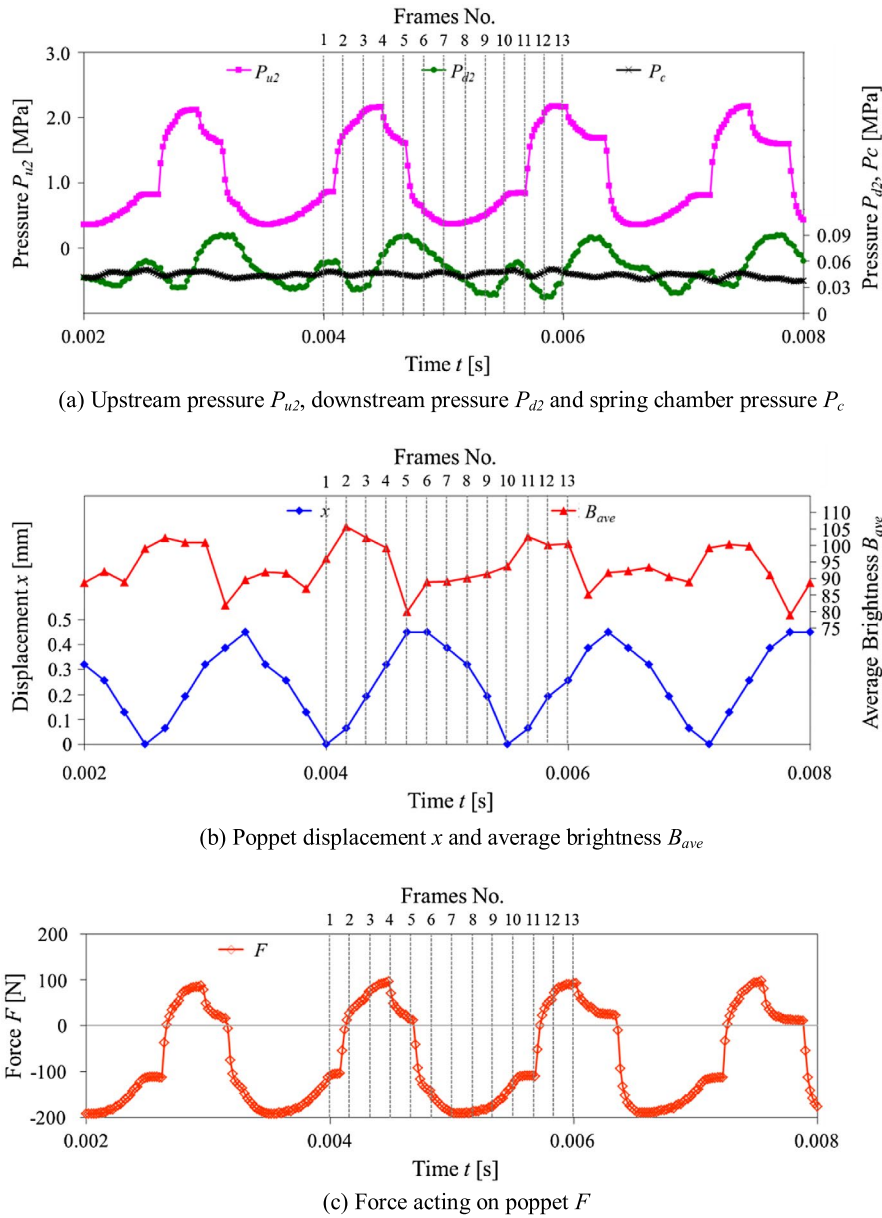


Figure 8. Correlation of factors at $Q=20\text{L/min}$ and $T=40^\circ\text{C}$; (a) upstream pressure P_{u2} , downstream pressure P_{d2} and spring chamber pressure P_c , (b) poppet displacement x and average brightness B_{ave} of the inspection area (quantity of cavitation bubbles), (c) force acting on the poppet F , calculated from measurements. The frame number refers to the images in Figure 9.

in the space. This is the cause of the increasing downstream pressure.

3.4. Mechanism of the poppet valve vibration

From the results of the previous sections, we constructed a hypothesis of the mechanism of the poppet valve vibration in the cavitation state. The mechanism shown in Figure 10 occurs in such a state. Specifically; (1) when the displacement of the poppet is small, there is cavitation and an annular vortex in the downstream portion; (2) because the oil has difficulty in flowing by the vortex and cavitation bubbles, discharge coefficient is reduced; (3) the upstream pressure increases with the decrease in discharge coefficient; (4) the poppet is

lifted by the increase in upstream pressure; (5) the flow rate increases with the opening area; (6) the vortex is released by increased flow rate; (7) because the oil is inhibited in its flow by the released vortex, downstream pressure increases between the poppet opening and the released vortex; (8) cavitation bubbles collapse owing to the greater downstream pressure, and bubbles thus disappear; (9) there is a switch to the flow field of the liquid phase only with the disappearance of bubbles, and fluid flows more easily because the discharge coefficient is recovered; (10) the upstream pressure decreases suddenly with the recovered discharge coefficient; (11) poppet displacement decreases with upstream pressure; and (12) the flow velocity increases at the throttle portion as the poppet displacement becomes smaller. Thereafter,

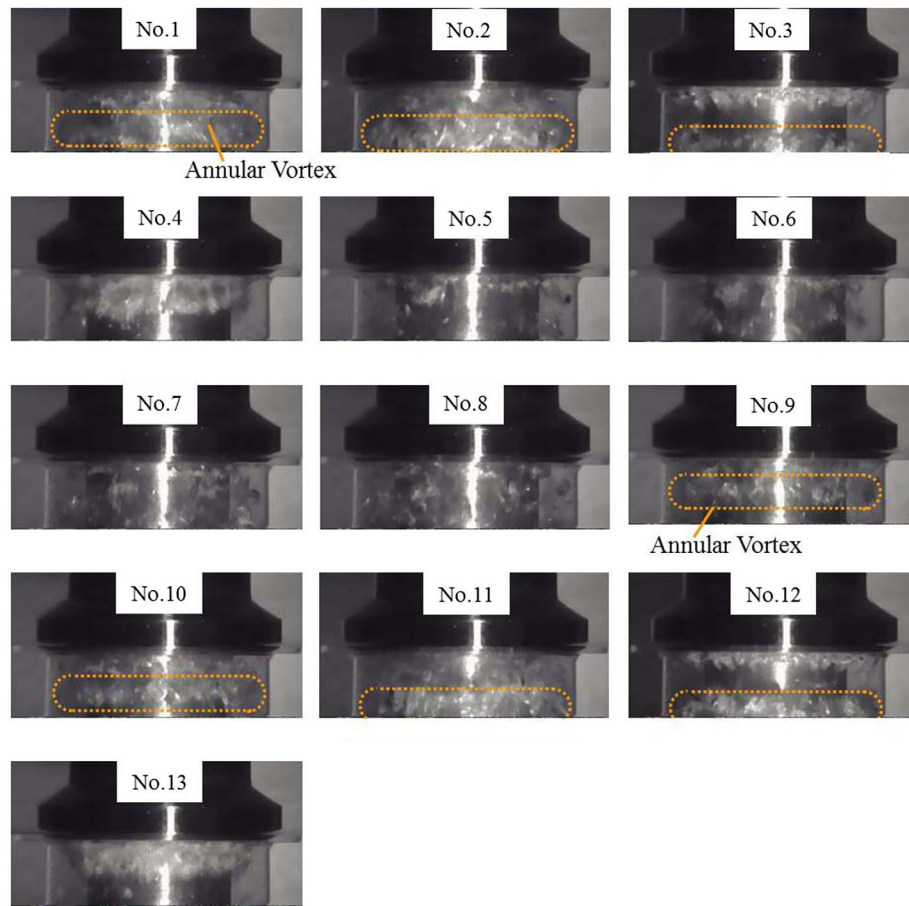


Figure 9. Transient state of cavitation for $Q=20\text{L/min}$ and $T=40\text{ }^\circ\text{C}$. The images present the state of cavitation corresponding to the frame numbers in Figure 8.

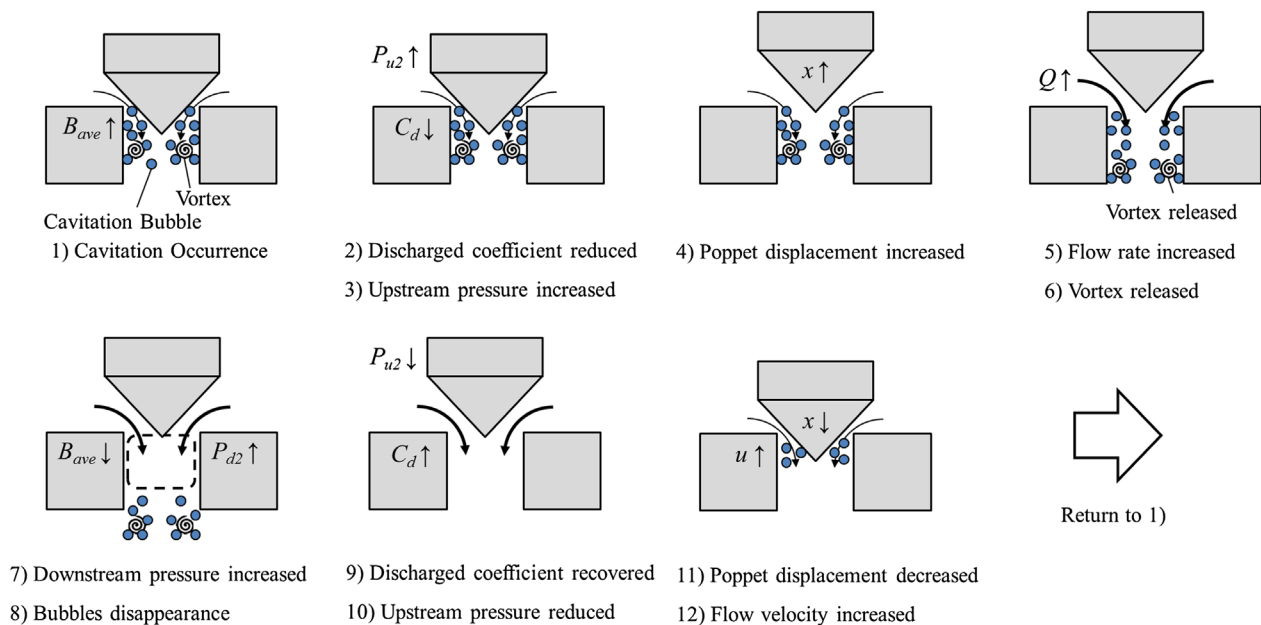


Figure 10. Mechanism of poppet valve vibration with cavitation phenomenon.

cycles of steps 1–11 are repeated. This hypothesis explains the facts observed from the experiments that the cavitation actually plays a role in amplifying the poppet valve vibration.

4. Conclusion

To explain how cavitation influences the vibration of a poppet valve, we carried out a series of high-speed

visualisation experiments. The vibration of the poppet valve was measured through image processing rather than by using an additional sensor for the poppet. According to the analysis of these experimental data, we proposed a hypothesis of the mechanism by which the vibration of the poppet valve occurs, based on the upstream pressure being excited because of the fluctuation of the quantity of cavitation bubbles and the behaviour of the annular vortex. This hypothesis explains the facts observed from the experiments that cavitation actually plays a function of role in amplifying the poppet valve vibration.

Disclosure statement

No potential conflict of interest was reported by the authors.

Notes on contributors



Kento Kumagai, born in 1984, received his Masters of Engineering from Muroran Institute of Technology in 2009. He has been a researcher at the Technical Research Laboratory of Hitachi Construction Machinery Co. Ltd since 2009. His main research area is the evaluation of the performance and flow state of hydraulic components. His current interest is the effect of bubbles in hydraulic systems and components.



Shohei Ryu, born in 1959, received his Masters degree from Zhejiang University in China in 1987, and a PhD from Saitama University in Japan in 1993. He joined Hitachi Construction Machinery Co. Ltd in 1993, and is now a senior researcher at the company's Technical Research Laboratory. His main research area is the performance evaluation of hydraulic components and power trains in construction machinery. His current interest is the review of old components with new investigation technology.



Masanori Ota received his Master of Engineering in 2003 and his Doctorate in Engineering degree in 2006 from the Graduate School of Science and Technology, Chiba University. He is an associate professor at Chiba University and his research interests are supersonic flow, optical measurement techniques and fluid mechanics.



Kazuo Maeno, born in 1949, graduated from the Department of Aeronautics at Tokyo University in 1974, and received his Masters and PhD (1979) from ISAS at Tokyo University. After starting his career at the Tokyo Metropolitan College of Aeronautical Engineering, he moved to Muroran Institute of Technology as an associate professor and then to Chiba University in 1990. In 2014, he became president of the National Institute of Technology Kisarazu College from vice dean of the Graduate School of Engineering of Chiba University.

ORCID

K. Maeno  <http://orcid.org/0000-0001-7382-0016>

References

- Backé, W. and Rünneburger, M., 1964. Zur Klärung des Verhaltens von Ueberdruckventilen [Clarify of behavior of pressure relief valve]. *Industrie anzeiger*, 88 (98), 2107–2116.
- Hayashi, S., 1995. Instability of poppet valve circuit. *JSME international journal series C*, 38 (3), 357–366.
- Knapp, R.T., Daily, J.W., and Hammit, F.G., 1970. *Cavitation*. New York: McGraw Hill.
- Kumagai, K., *et al.*, 2014a. Renewed study of vibration phenomenon in poppet type valve. In: H. Murrenhoff, ed. *Proceedings of the 9th international fluid power conference 9*, IFK, 24–26 March 2014 Aachen. Aachen: RWTH Aachen University, 2, 80–91.
- Kumagai, K., *et al.*, 2014b. Vibration phenomenon of poppet valve in hydraulic system – relationship between poppet valve vibration and cavitation phenomenon. *The journal of JFPS*, 45 (6), 94–100, in Japanese.
- Lutz, O., 1933. Die Vorgänge in federbelasteten Einspritzdüsen von kompressorlosen Ölmaschinen [Operations of spring-loaded injector in dieselmotor]. *Ingenieur-Archiv*, 4 (2), 153–168.
- Maeda, T., 1970. Studies on the dynamic characteristic of a poppet valve: 1st report, theoretical analysis. *Bulletin of JSME*, 13 (56), 281–289.
- Oshima, S. and Ichikawa, T., 1986. Cavitation phenomena and performance of oil hydraulic poppet valve: 3rd report, influence of the poppet angle and oil temperature on the flow performance. *Bulletin of JSME*, 29 (249), 743–750.
- Weaver, D.S., 1980. Flow-induced vibrations in valves operating at small openings. In: E. Naudascher and D. Rockwell, eds. *Practical experiences with flow-induced vibrations*. Berlin: Springer-Verlag, 305–319.